Probing the properties of nebular plasmas with optical and infrared spectroscopy

M. J. Barlow

Citation: AIP Conf. Proc. **1438**, 103 (2012); doi: 10.1063/1.4707863
View online: http://dx.doi.org/10.1063/1.4707863
View Table of Contents: http://proceedings.aip.org/dbt/dbt.jsp?KEY=APCPCS&Volume=1438&Issue=1
Published by the American Institute of Physics.

Probing the properties of nebular plasmas with optical and infrared spectroscopy

M. J. Barlow

Dept. of Physics and Astronomy, University College London, London WC1E 6BT, U.K.

Abstract. A number of current developments arising from spectroscopic studies of ionized nebulae are reviewed. Until the past decade or so, such studies were generally confined to the analysis of recombination lines from hydrogen and helium, along with collisionally excited forbidden lines from second and third row elements in the periodic table. However, the advent of efficient detectors on 8m-class telescopes has enabled the detection of recombination lines from second and third row elements, along with collisionally excited lines from much less abundant species. Significant discrepancies have been found between ionic abundances derived from collisionally excited lines and those obtained for the same ions from their recombination lines. The existence of 'cold plasma' with $T_e \leq 1000$ K has been confirmed for a number of planetary nebulae. Optical and infrared collisionally excited ionic lines from a wide range of 'neutron-capture' elements from beyond the iron abundance peak have also been detected. There is a consequent need for new calculations and experimental measurements of the atomic data needed to interpret these observations.

Keywords: Nebulae, Atomic Processes, Spectroscopy
PACS: 95.30.Ky,98.38.Bn,98.38.Ly

INTRODUCTION

There are two main classes of photoionized nebulae, H II regions and planetary nebulae. The brightest examples of H II regions are the result of the formation of massive stars (> 20 $M_\odot$), which then ionise and disperse their natal clouds. The ionising stars have temperatures of 25,000 K $< T_{star} <$ 50,000 K. Planetary Nebulae (PNe) are the final stage in the lives of low and intermediate mass stars, before they become white dwarfs. The outer envelope is ejected during the red giant Asymptotic Giant Branch (AGB) phase and then photoionised by a hot remnant star with 25,000 K $< T_{star} <$ 220,000 K, with the result that many PNe exhibit much higher degrees of ionization than do H II regions, which rarely show emission from doubly ionized helium, a species that is common in PNe.

Typical proton and electron densities in ionized nebulae range between 1 - 10^5 cm^{-3}. The abundance of helium is 10% that of hydrogen, by number, while the next most abundant element is oxygen (5×10^{-4} the abundance of hydrogen). Any elements other than H and He are referred to as 'heavy elements' or 'metals'. The very low ambient densities and low electron collision rates in nebulae mean that many heavy element excited state decays that are electric dipole-forbidden have enough time to decay by magnetic dipole or electric quadrupole transitions. Such emission lines are called 'forbidden lines' or 'collisionally excited lines' (CELs).

The 17th International Conference on Atomic Processes in Plasmas (ICAPiP)
AIP Conf. Proc. 1438, 103-110 (2012); doi: 10.1063/1.4707863

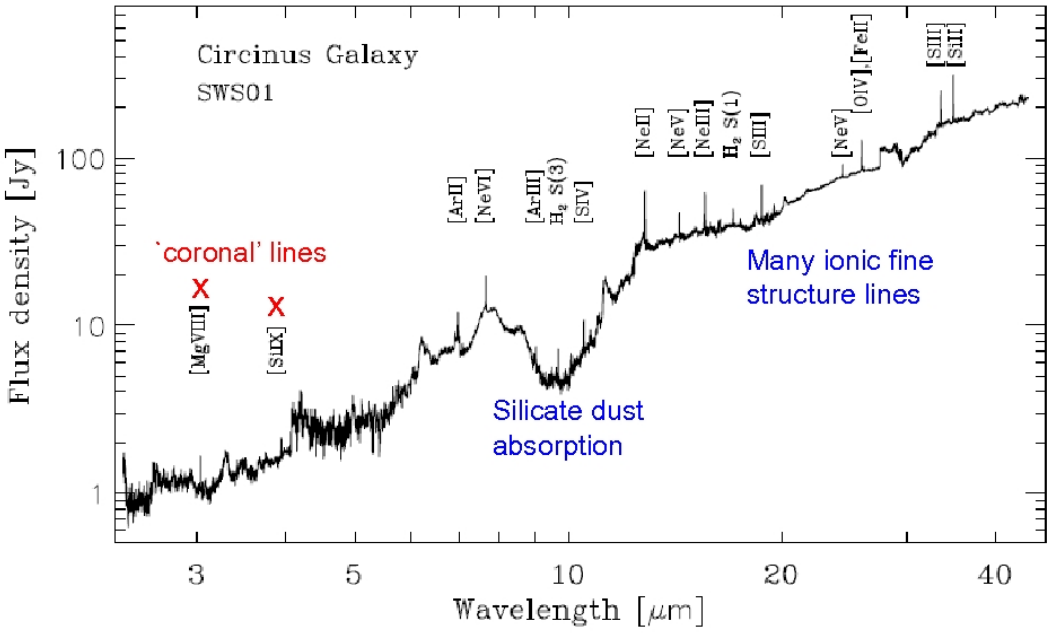

FIGURE 1. An annotated version of the 2.4-45.0-μm ISO SWS spectrum of the Circinus Galaxy published by Moorwood et al. [18]. This galaxy hosts an X-ray emitting massive central black hole whose radiation is responsible for the highly ionized species of neon, magnesium and silicon that exhibit emission lines in this spectrum.

Along with hydrogen and helium recombination lines, forbidden lines of C, N, O and Ne dominate the UV, optical and infrared spectra of ionized nebulae. In the optical and UV spectral regions, their large excitation energies make them very sensitive to the local electron temperature. On the other hand infrared ground-state fine-structure forbidden lines have low excitation energies and so are insensitive to the local electron temperature. Another advantage of observing in the infrared is that the effects of dust obscuration decrease strongly with increasing wavelength, enabling regions that are heavily obscured in the optical to be revealed at infrared wavelengths, e.g. regions of massive star formation, or dusty tori around accreting massive black holes in active galactic nuclei. As an example of the latter, Figure 1 shows the 2.4-45.0-μm Infrared Space Observatory spectrum of the Circinus Galaxy, which exhibits a very large number of IR fine structure lines, including 'coronal' lines of highly ionized silicon and magnesium that have been produced by the very hard UV and X-ray power-law spectrum from the central engine. A very good overview of the processes at work in astrophysical ionized nebulae can be found in the monograph by Osterbrock and Ferland [19].

The advent of 8-10m class telescopes equipped with very sensitive spectrographs and large format detectors has enabled the detection of large numbers of extremely faint emission lines from ionized nebulae, for example the 3500-9865 Å optical echelle spectrum of the narrow-lined planetary nebula IC 418 presented by Sharpee et al. [25], in which over 800 emission lines were detected down to intensities less than 10^{-5} of the

Hβ recombination line of hydrogen. Spectra of this type have enabled the detection of many optical recombination lines (ORLs) from second-row elements such as C, N, O and Ne, as well as from third-row elements such as Mg, Si and S. In addition, collisionally excited forbidden lines can be detected from even less abundant elements that are beyond the 'iron-peak' limit for element production by fusion reactions. These elements are produced by 'slow' (s-process) neutron capture reactions that take place in the envelopes of AGB red giant stars just before the creation of a planetary nebula.

OPTICAL RECOMBINATION LINE (ORL) ABUNDANCES VS. COLLISIONALLY EXCITED LINE (CEL) ABUNDANCES

The strong Boltzmann factor dependence of optical and UV CELs makes them very sensitive to temperature fluctuations within a nebula, as noted by Peimbert [21], who developed the widely used t^2 root mean square temperature fluctuation formalism to describe this phenomenon. Fig. 2 shows that IR fine structure lines are insensitive to temperature and to temperature fluctuations, but unfortunately it is often difficult to compare optical spectroscopic measurements of H II regions with IR spectroscopic observations, due to the very different apertures that are often used (this is not the case for planetary nebulae, which are usually compact enough for line fluxes for an entire nebula to be measured in both wavelength regions). Fig. 2 also shows the sensitivity to electron density of the [O III] 52-μm line, which has a critical density of $\sim$5000 cm^{-3} (the electron density at which radiative decay rates out of the upper level are equal to the sum of the upward and downward collisional rates out of the same level). The [O III] 88-μm line has a critical density of $\sim$500 cm^{-3}, so the 52/88-μm line ratio is a sensitive density diagnostic for many ionized nebulae.

Deriving the abundance of a particular element in a nebula requires a summation of the abundances of all of its ion stages, not all of which may be observationally accessible. Two remedies are available: (a) the application of 'ionization correction factors' (ICFs) to allow for missing ion stages, based on the use of other elements that have observable ion stages with similar ionization potential to those that are missing. An example of this is the ICF scheme of Kingsburgh and Barlow [11]; (b) the calculation of a tailored numerical radiative transfer model to estimate the relative abundances of all ion stages of each element in a nebula. The most widely used code is CLOUDY, originated by G. J. Ferland and collaborators. Other nebular radiative transfer codes include MAPPINGS (M. Dopita, L. Binette, R. Sutherland and collaborators) and the 3D Monte Carlo code MOCASSIN (B. Ercolano and collaborators). These codes make use of photoionization cross-sections, recombination rates (radiative and dielectronic) and charge transfer rates for many different ions, obtained from many sources. Queen's University Belfast, the Iron Project and the APAP network have played a leading role in providing such data. A model for the energy distribution of the central star is also required (NLTE, wind-blanketed, etc.).

Optical recombination lines (ORLs) and collisionally excited lines (CELs) can be measured at optical wavelengths in the same spectrum, and the closely similar T_e de-

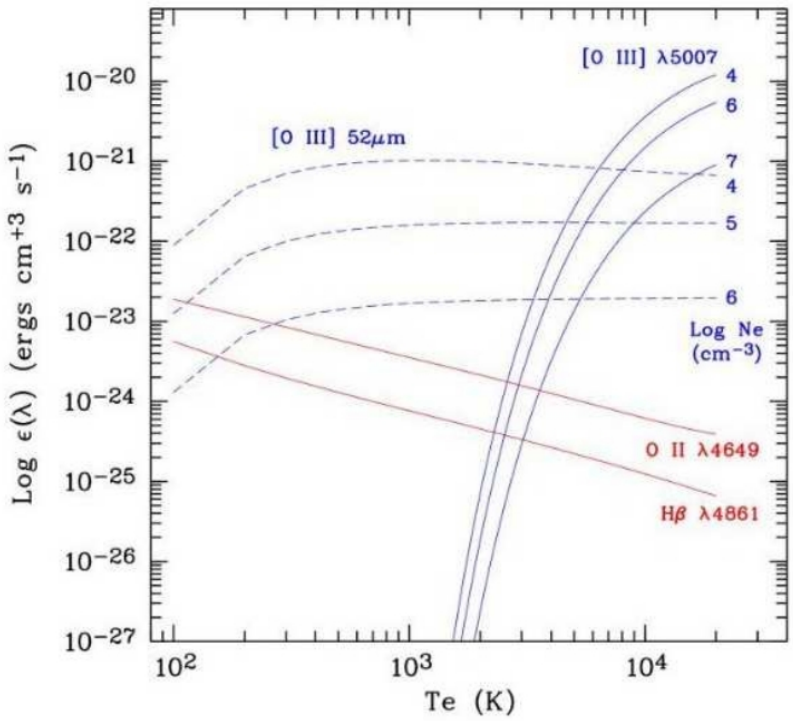

FIGURE 2. An illustration of the dependence on electron temperature T_e (and electron density N_e) of several classes of nebular emission lines. Top (solid) curves: the emissivity of the [O III] 5007 Å line as a function of T_e (based on the O^{2+} collision strengths of Aggarwal [1], for the three different values of electron density (log N_e) indicated by the labels. Middle (dashed) curves: the emissivity of the [O III] 52-μm line for three different values of log N_e. Bottom (solid) curves: the temperature dependence of the emissivities of the O II 4649 Å and Hβ recombination lines. Via the Boltzmann factor term, the relatively large excitation energy of the strong [O III] 5007 Å optical CEL gives it a very steep dependence on T_e, for typical nebular nebular temperatures. Due to the much smaller excitation energy of the 52-μm [O III] infrared fine structure line, it has a very weak dependence on T_e. The inverse T_e dependence of the O II 4649 Å recombination line is nearly the same as that of hydrogen recombination lines such as Hβ, so ORL ionic abundances relative to H^+ ought to have virtually no sensitivity to T_e.

pendences of heavy element and hydrogen recombination lines (Figure 2) should cause ORL ionic abundances to be insensitive to nebular temperature fluctuations. As a result, deep high signal to noise spectra have been obtained for many nebulae over the past 15 years using the latest generation of telescopes and their associated instrumentation, with sometimes surprising results.

H II Regions

Deep optical spectra of a significant number of bright Galactic and extragalactic H II regions have been obtained by e.g. Esteban et al. [6], Peimbert [20], Tsamis et al. [31], Garcia-Rojas et al. [9], Garcia-Rojas and Esteban [10] and Esteban et al. [7], yielding

good S/N detections of a large number of ORLs from O II and other ions. Tsamis et al. [32] introduced the abundance discrepancy factor (ADF), which they defined as the ratio of the ORL abundance of an ion to the CEL abundance of the same ion. Typical H II region ADFs of about a factor of two are found. This level of discrepancy can be accounted for by relatively modest temperature fluctuations ($t^2 \sim 0.03 - 0.04$), with a number of studies indicating that the effects of flows from embedded Herbig-Haro objects and proplyds (both due to embedded protostars) may be able to account for the observed level of discrepancy [17, 34]. The inference is that in the case of H II regions the (larger) ORL heavy element abundances should be preferred over those from the traditional CEL technique.

Planetary Nebulae

In the case of planetary nebulae, deep spectroscopic observations of ORLs and CELs have shown that while most ADFs are between 2 and 3, a significant number of PNe have much higher ADFs [12, 13, 14, 15, 32, 33, 16, 36, 37, 38]. For example, the Saturn Nebula, NGC 7009, was found to have an ADF of 4.7 by Liu et al. [12], a T_e([O III]) of 9980 K, a H I Balmer Jump temperature of 8150 K, a T_e from He I recombination line ratios of 5380 K and an O II recombination line ratio T_e of 1800 K. Hf 2-2, a PN with one of the highest known overall nebular ADF values (84), was found to have T_e's of 8820, 900, 775 and 360 K from the same four diagnostics [15].

Temperature fluctuations [21] or density inhomogeneities [24, 35] cannot explain the factors of ten or more discrepancies between ORL and CEL abundances measured for some planetary nebulae. A clue to the cause of these large ADFs comes from observations of the spatially resolved hydrogen-deficient knots in the planetary nebula Abell 30, for which empirical analysis [36] and 3-D photoionization modelling [5] yielded ADFs of 300-700; the strong ORLs were found to originate from cold plasma ($T_e < 3000$ K). Normally the primary heating mechanism in a nebula is photoionization of hydrogen but if hydrogen is depleted then photoelectron ejection from grain surfaces can become the dominant heating mechanism [2]. For a H-dominated nebula, collisionally excited optical forbidden lines provide the dominant cooling mechanism but if H is depleted then infrared collisionally excited lines can alone suffice to balance the heating rate from grain photoelectron ejection. Since IR CELs have low excitation energies, equilibrium plasma electron temperatures of 1000 K or less are therefore possible.

Relative to nebular forbidden-line T_e's, the lower nebular T_e's that are derived from Balmer Jump measurements, and from He I and O II recombination line ratios, suggest that high-ADF nebulae contain at least two distinct emission regions: (1) a 'normal' component with a 'normal' temperature ($T_e \sim 10^4$ K) and 'normal' abundances, from which the strong CELs originate; (2) a 'hydrogen-deficient' component, with a low temperature ($T_e \sim 10^3$ K) and very high heavy element abundances. This component would emit most of the observed flux from the heavy element ORLs but essentially

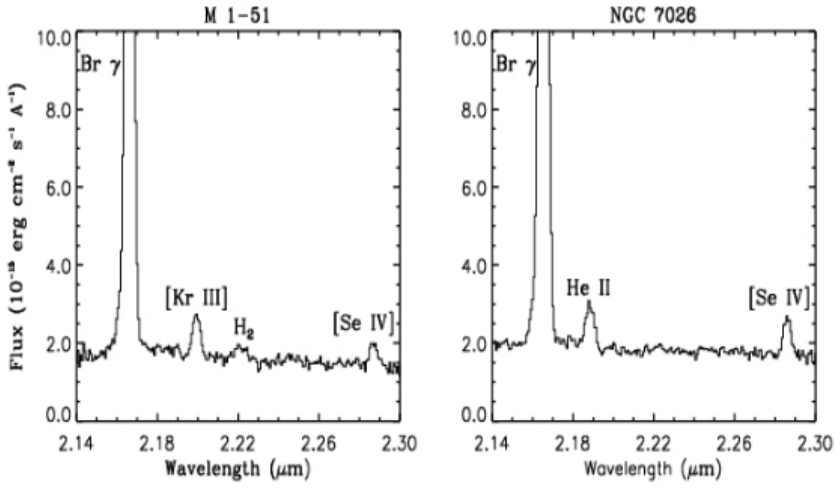

FIGURE 3. The 2-μm spectra of two planetary nebulae that show s-process element ionic forbidden line emission, namely the 2.199-μm line of [Kr III] and the 2.287-μm line of [Se IV]. From Sterling and Dinerstein [28].

no optical CEL emission. In this scenario, ORLs and CELs yield different element abundances simply because they trace two completely different ionized regions, with the ORLs revealing a new nebular component, cold plasma enriched in heavy elements. The origin of the posited H-deficient component is still unknown. It appears that the 'normal' gas is the dominant mass component in PNe, with CELs providing reliable heavy element abundance estimates for this component.

NEUTRON-CAPTURE ELEMENTS IN PLANETARY NEBULAE

Elements beyond the 'iron peak' cannot be made by nuclear fusion reactions. Instead they are synthesised by neutron captures by 'seed' nuclei' that were made by fusion reactions during earlier cycles of stellar evolution. These neutron capture elements can be made by two processes [3] - by rapid or 'r-process' neutron captures in core-collapse supernovae, or by slow or 's-process' neutron captures that take place in the envelopes of intermediate mass AGB stars. In the solar system, s-process elements and isotopes dominate elemental abundances beyond the iron peak. A great deal of theoretical work has been carried out to predict abundances for neutron-capture elements, and although these predictions can be tested for some elements, whose lines are detectable in the spectra of late-type stars, many elements remain observationally inaccessible outside the solar system. Since planetary nebulae are formed from the envelopes of AGB stars, they ought to provide ideal laboratories for testing models for the formation of neutron-capture elements. However, in the past two factors have combined to make their study difficult: (1) their low cosmic abundances (typically $< 4 \times 10^{-9}$ of the abundance of hydrogen) mean that even their collisionally excited lines will be very weak; (2) the atomic data needed for abundance estimation is often poorly known. The availability of deep optical and infrared spectra from large telescopes has begun to deal with the first

effect, while efforts are now underway to ameliorate the second factor.

Péquignot & Baluteau [23] identified two long unidentified lines in the optical spectrum of the bright PN NGC 7027 as [Kr IV] lines. A dozen ions belonging to Kr, Xe, Br, Se, Rb, and Ba were also identified by them in the spectrum. Dinerstein [4] identified two emission lines that had been often seen in the 2-μm spectra of planetary nebulae, as [Kr III] 2.199 μm and [Se IV] 2.287 μm, both ions of s-process elements (see Figure 3). Sterling et al. [27, 28] carried out a near-IR spectral survey of 120 planetary nebulae, yielding 81 detections of Kr/Se, representing a factor of 10 increase in the number of PNe with neutron-capture element detections. Sharpee et al. [26] and Sterling et al. [29] have reported deep optical echelle spectroscopy of 4 and 17 planetary nebulae, respectively, leading to the detection of ions of Kr, Xe, Br, Se, Rb, Ba and Pb.

To complement these line detections, good quality atomic data are needed, not just transition probabilities and collisional cross-sections, to enable the derivation of the abundances of the observed ions, but also photoionization cross-sections, recombination rate coefficients (both radiative and dielectronic) and charge transfer rates, so that nebular photoionization models can be constructed to allow the estimation of the relative abundances of both observed and unseen ion stages. To address these issues, N. Sterling has formed a collaboration which has calculated, or measured experimentally, a number of the required datasets. Sterling and Witthoeft [30] produced multi-configuration Breit-Pauli AUTOSTRUCTURE calculations of distorted-wave photoionization cross sections, along with total and partial final-state resolved radiative recombination and dielectronic recombination rate coefficients for the first six ions of the trans-iron element selenium. Esteves et al. [8] made use of the Advanced Light Source (ALS) at Lawrence Berkeley National Laboratory, using the photo-ion merged-beams technique to measure absolute photoionization cross-section measurements for Se^+ ions, including their complex resonant structure.

FUTURE REQUIREMENTS

Much of the recent focus of atomic data calculations and measurements has been on the highly charged ions found in X-ray emitting plasmas, with a consequent neglect of the relatively low-charged ions found in nebular plasmas. With the ever-increasing number of detections of nebular recombination lines from second and third row elements, as well as of many ionic forbidden lines from elements beyond the iron peak, there is now an urgent requirement for complementary atomic datasets, in order to probe the physical and chemical structures of nebulae and to obtain the abundances of neutron-capture elements in a range of environments outside the solar system, thereby providing observational probes of the formation mechanisms of many of these elements for the first time.

REFERENCES

1. K. M. Aggarwal, *ApJS*, **52**, 387 (1983).
2. K. J. Borkowski, J. P. Harrington, Z. Tsvetanov and R. E. S. Clegg, *ApJ*, **415**, L47 (1993).
3. E. M. Burbidge, G. R. Burbidge, W. A. Fowler and F. Hoyle, *RevModPhys*, **29**, 547 (1957).
4. H. L. Dinerstein, *ApJ*, **550**, L223 (2001).
5. B. Ercolano, M. J. Barlow, P. J. Storey, X.-W. Liu, T. Rauch and K. Werner, *MNRAS*, **344**, 1145 (2003).
6. C. Esteban, M. Peimbert, S. Torres-Peimbert and M. Rodriguez, *ApJ*, **581**, 241 (2002).
7. C. Esteban, F. Bresolin, M. Peimbert, H. Garcia-Rojas, A. Peimbert and A. Mesa-Delgado, *ApJ*, **700**, 654 (2009).
8. D. A. Esteves, et al. *PhysRevA*, **84**, 013406 (2011).
9. J. Garcia-Rojas, C. Esteban, A. Peimbert, M. Peimbert, M. Rodriguez and M. T. Ruiz, *MNRAS*, **362**, 301 (2005).
10. J. Garcia-Rojas and C. Esteban, *ApJ*, **670**, 457 (2007).
11. R. L. Kingsburgh and M. J. Barlow, *MNRAS*, **271**, 257 (1994).
12. X.-W. Liu, P. J. Storey, M. J. Barlow and R. E. S. Clegg, *MNRAS*, **272**, 369 (1995).
13. X.-W. Liu, P. J. Storey, M. J. Barlow, I. J. Danziger, M. Cohen and M. Bryce, *MNRAS*, **312**, 585 (2000).
14. X.-W. Liu, S.-G. Luo, M. J. Barlow, I. J. Danziger and P. J. Storey, *MNRAS*, **327**, 141 (2001).
15. X.-W. Liu, M. J. Barlow, Y. Zhang, R. J. Bastin and P. J. Storey, *MNRAS*, **368**, 1959 (2006).
16. Y. Liu, X.-W. Liu, M. J. Barlow and S.-G. Luo, *MNRAS*, **353**, 1231 (2004).
17. A. Mesa-Delgado, L. Lopez-Martin, C. Esteban, J. Garcia-Rojas and V. Luridiana, *MNRAS*, **394**, 693 (2009).
18. A. F. M. Moorwood, et al., *A&A*, **315**, L105 (1996).
19. D.E. Osterbrock and G.J. Ferland, *Astrophysics of Gaseous Nebulae and Active Galactic Nuclei, 2nd. ed.* University Science Books, Sausalito, (2006).
20. A. Peimbert, *ApJ*, **584**, 735 (2003).
21. M. Peimbert, *ApJ*, **150**, 825 (1967).
22. M. Peimbert, A. Peimbert, C. Esteban, J. Garcia-Rojas, F. Bresolin, L. Carigi, M. T. Ruiz and A. R. Lopez-Sanchez, *RevMexAA*, **100**, 500 (2006).
23. D. Péquignot and J. P. Baluteau, *A&A*, **283**, 593 (1994).
24. R. H. Rubin, *ApJS*, **69**, 897 (1989).
25. B. Sharpee, J. A. Baldwin and R. E. Williams, *ApJ*, **615**, 323 (2004).
26. N. Sharpee, Y. Zhang, R. E. Williams, Pellegrini, K. Cavagnolo, J. A. Baldwin, M. Phillips and X.-W. Liu, *ApJ*, **659**, 1265 (2007).
27. N. C. Sterling, H. L. Dinerstein and T. R. Kallman, *ApJS*, **169**, 37 (2007).
28. N. C. Sterling and H. L. Dinerstein, *ApJS*, **174**, 158 (2008).
29. N. C. Sterling, et al., *PASA*, **26**, 339 (2009).
30. N. C. Sterling and M. C. Witthoeft, *A&A*, **529**, 147 (2011).
31. Y. G. Tsamis, M. J. Barlow, X.-W. Liu, I. J. Danziger and P. J. Storey, *MNRAS*, **338**, 687 (2003).
32. Y. G. Tsamis, M. J. Barlow, X.-W. Liu, P. J. Storey and I. J. Danziger, *MNRAS*, **353**, 953 (2004).
33. Y. G. Tsamis, J. R. Walsh, D. Péquignot, M. J. Barlow, I. J. Danziger and X.-W. Liu, *MNRAS*, **386**, 22 (2008).
34. Y. G. Tsamis, J. R. Walsh, J. M. Vilchez and D. Péquignot, *MNRAS*, **412**, 1367 (2011).
35. S. M. Viegas and R. E. S. Clegg, *MNRAS*, **271**, 993 (1994).
36. R. Wesson, X.-W. Liu and M. J. Barlow, *MNRAS*, **340**, 253 (2003).
37. R. Wesson, X.-W. Liu and M. J. Barlow, *MNRAS*, **362**, 424 (2005).
38. R. Wesson, M. J. Barlow, X.-W. Liu, P. J. Storey, B. Ercolano and O. De Marco, *MNRAS*, **383**, 1639 (2008).